Loop corrections to pion and kaon neutrinoproduction

Marat Siddikov, Iván Schmidt
Departamento de Física, Universidad Técnica Federico Santa María,
y Centro Científico - Tecnológico de Valparaíso, Casilla 110-V, Valparaíso, Chile

In this paper we study the next-to-leading order corrections to deeply virtual pion and kaon production in neutrino experiments. We estimate these corrections in the kinematics of the MINERVA experiment at FERMILAB, and find that they are sizable and increase the leading order cross-section by up to a factor of two. We provide a computational code, which can be used for the evaluation of the cross-sections, taking into account these corrections and employing various GPD models.

arXiv:1611.07294v1 [hep-ph] 22 Nov 2016

I. INTRODUCTION

Today generalized parton distributions (GPDs) are used as a common language to parametrize the nonperturbative structure of the target. In Bjorken kinematics, due to collinear factorization theorems [1, 2], these objects can be accessed in a study of cross-sections for a wide class of processes. Nowadays all the information on GPDs comes from the electron-proton and positron-proton measurements done at JLAB and HERA, in particular deeply virtual Compton scattering (DVCS) and deeply virtual meson production (DVMP) [1–16]. However, due to the rich structure of GPDs, as well as the limited available experimental data, modern parametrizations of GPDs still rely significantly on various additional assumptions. A planned CLAS12 upgrade at JLAB will improve our understanding of GPDs and will extend the kinematic coverage [16]. Nevertheless, the flavor structure of GPDs has been experimentally tested only for limiting cases, PDFs and form factors, and its extrapolation to a broader kinematical range still rests on additional implicit assumptions. This happens because DVCS alone only probes a certain flavor combination, whereas analysis of eDVMP is aggravated by large uncertainties from twist-3 effects for pion production [16–20] and from lack of knowledge of meson distribution amplitudes (DAs) for vector meson production.

Earlier [21] we suggested that GPDs could be studied in neutrino-induced deeply virtual meson production (νDVMP) of the pseudo-Goldstone mesons (π, K, η), using the high-intensity NUMI beam at Fermilab. Right now it runs in the so-called middle-energy (ME) regime, with an average neutrino energy of about 6 GeV, although without major rebuild potentially it could deliver neutrinos with energies up to 20 GeV [22]. For studies of flavor structure, νDVMP has a clear advantage compared to *electro*production: since in addition to the vector channel, which is sensitive to a small helicity flip GPDs $\tilde{H}$ and $\tilde{E}$, and easily gets shadowed by twist-3 effects [16] at moderate virtualities Q^2, the axial part of the weak current gets large contributions from the unpolarized GPDs, H, E. As we have shown earlier [23], in the case of νDVMP, due to these contributions, the admixture of twist-3 terms becomes negligible [1]. An additional appeal of the axial channel stems from the closeness of pion and kaon distribution amplitudes, guaranteed by chiral symmetry breaking: neglecting the difference of masses of the two goldstones in Bjorken kinematics, we may consider the final state mesons as natural filters of the different GPDs flavor combinations. A suppression of Cabibbo forbidden, strangeness changing processes can be avoided if kaon production is accompanied by the conversion of a nucleon to strange baryons Λ and $\Sigma^{\pm,0}$: in such processes the transition GPDs are related by $SU(3)$ relations [25] to linear combinations of different flavor components of the nucleon GPDs. If all the suggested channels will be measured by MINERvA, a full light flavor structure of nucleon GPDs could be extracted. Recently it was suggested in [26–28] that this approach could be extended to D-meson production, a challenge for future high-energy neutrino experiments. However, that kinematics analysis is more complicated due to additional Bethe-Heitler type corrections [29], which are small in MINERvA kinematics, but grow with Q^2 and eventually become the dominant mechanism. Moreover, the fact that nuclear targets are used in neutrino experiments does not introduce significant uncertainty if we consider incoherent scattering at sufficiently large recoil momenta $|t| \gg R_A^{-2}$, where R_A is the nuclear radius [30].

Given the potential of neutrinoproduction of goldstone mesons for proton structure studies, in this paper we proceed with the corresponding analysis and evaluate the next-to-leading order (NLO) corrections to DVMP. As we will show below, for the kinematics of ongoing and forthcoming neutrino experiments, where typical virtualities Q^2 are not very large, the NLO corrections are significant and affect the analysis of the DVMP contributions. The paper is organized as follows. In Section II we evaluate the goldstone meson production by neutrinos on nucleon targets, taking into account higher twist effects. In Section III, for the sake of completeness, we sketch the properties of the GPDs parametrization which will be used for evaluations. In Section IV we present numerical results and conclusions.

[1] In this respect we differ from [24], where it was assumed that the twist-3 contribution is the dominant mechanism.

II. CROSS-SECTION OF THE νDVMP PROCESS

The cross-section of goldstone mesons production in neutrino-hadron collisions has a form

$$\frac{d\sigma}{dt\,dx_B dQ^2} = \Gamma \sum_{\nu\nu'} \mathcal{A}^*_{\nu',\nu L}\mathcal{A}_{\nu',\nu L}, \tag{1}$$

where $t = (p_2 - p_1)^2$ is the momentum transfer to the baryon, $Q^2 = -q^2$ is the virtuality of the charged boson, $x_B = Q^2/(2p\cdot q)$ is the Bjorken variable, the subscript indices ν and ν' in the amplitude $\mathcal{A}$ refer to helicity states of the baryon before and after interaction, and the letter L reflects the fact that in the Bjorken limit the dominant contribution comes from the longitudinally polarized massive bosons $W^\pm/Z$ [1, 2]. The kinematic factor Γ in (1) is different for charged current and neutral current processes and is given explicitly by

$$\Gamma_{CC} = \frac{G_F^2 f_M^2 x_B^2 \left(1 - y - \frac{\gamma^2 y^2}{4}\right)}{64\pi^3 Q^2 \left(1 + Q^2/M_W^2\right)^2 (1+\gamma^2)^{3/2}}, \tag{2}$$

$$\Gamma_{NC} = \frac{G_F^2 f_M^2 x_B^2 \left(1 - y - \frac{\gamma^2 y^2}{4}\right)}{64\pi^3 \cos^4\theta_W Q^2 \left(1 + Q^2/M_Z^2\right)^2 (1+\gamma^2)^{3/2}}. \tag{3}$$

where θ_W is the Weinberg angle, M_W and M_Z are the masses of the heavy bosons $W^\pm$ and M_Z, G_F is the Fermi constant, f_M is the produced meson (pion or kaon) decay constant, and we have introduced the shorthand notations

$$\gamma = \frac{2\,m_N x_B}{Q}, \quad y = \frac{Q^2}{s_{\nu p}\,x_B} = \frac{Q^2}{2m_N E_\nu\,x_B}. \tag{4}$$

where E_ν is the neutrino energy in the target rest frame.

Thanks to the factorization theorem, the amplitude $\mathcal{A}_{\nu',\nu L}$ in (1) may be written as a convolution of hard and soft parts,

$$\mathcal{A}_{\nu',\nu L} = \int_{-1}^{+1} dx \sum_{q,q'=u,d,s,g} \sum_{\lambda\lambda'} \mathcal{H}^{q'q}_{\nu'\lambda',\nu\lambda} \mathcal{C}^{q'q}_{\lambda',\lambda L}, \tag{5}$$

where x is the average light-cone fraction of the parton, λ, q (λ', q') are the corresponding helicity and flavor of the initial (final) partons, and $\mathcal{C}^q_{\lambda'\nu',\lambda\nu}$ is the hard coefficient function, which will be specified later. The soft matrix element $\mathcal{H}^q_{\nu'\lambda',\nu\lambda}$ in (9) is diagonal in quark helicities (λ,λ'), at leading twist,

$$\begin{aligned}\mathcal{H}^{q'q}_{\nu'\lambda',\nu\lambda} = \frac{2\delta_{\lambda\lambda'}}{\sqrt{1-\xi^2}} \Bigg(& -g_A^q \begin{pmatrix} \left(1-\xi^2\right) H^{q'q} - \xi^2 E^{q'q} & \frac{(\Delta_1 + i\Delta_2) E^{q'q}}{2m} \\ -\frac{(\Delta_1 - i\Delta_2) E^{q'q}}{2m} & \left(1-\xi^2\right) H^{q'q} - \xi^2 E^{q'q} \end{pmatrix}_{\nu'\nu} \\ & + \mathrm{sgn}(\lambda) g_V^q \begin{pmatrix} -\left(1-\xi^2\right) \tilde{H}^{q'q} + \xi^2 \tilde{E}^{q'q} & \frac{(\Delta_1 + i\Delta_2)\xi \tilde{E}^{q'q}}{2m} \\ \frac{(\Delta_1 - i\Delta_2)\xi \tilde{E}^{q'q}}{2m} & \left(1-\xi^2\right) \tilde{H}^{q'q} - \xi^2 \tilde{E}^{q'q} \end{pmatrix}_{\nu'\nu} \Bigg),\end{aligned} \tag{6}$$

where the constants g_V^q, g_A^q are the vector and axial current couplings to quarks, and the four leading twist GPDs $H^{q'q}$, $E^{q'q}$, $\tilde{H}^{q'q}$ and $\tilde{E}^{q'q}$ are defined as

$$\begin{aligned}\frac{\bar{P}^+}{2\pi} \int dz\, e^{ix\bar{P}^+ z} \left\langle B(p_2) \left| \bar{\psi}_{q'}\left(-\frac{z}{2}\right) \gamma_+ \psi_q\left(\frac{z}{2}\right) \right| A(p_1) \right\rangle &= \Big(H^{q'q}(x,\xi,t)\, \bar{N}(p_2)\, \gamma_+ N(p_1) \\ &\quad + \frac{\Delta_k}{2m_N} E^{q'q}(x,\xi,t)\, \bar{N}(p_2)\, i\sigma_{+k} N(p_1) \Big)\end{aligned} \tag{7}$$

$$\begin{aligned}\frac{\bar{P}^+}{2\pi} \int dz\, e^{ix\bar{P}^+ z} \left\langle B(p_2) \left| \bar{\psi}_{q'}\left(-\frac{z}{2}\right) \gamma_+\gamma_5 \psi_q\left(\frac{z}{2}\right) \right| A(p_1) \right\rangle &= \Big(\tilde{H}^{q'q}(x,\xi,t)\, \bar{N}(p_2)\, \gamma_+\gamma_5 N(p_1) \\ &\quad + \frac{\Delta_+}{2m_N} \tilde{E}^{q'q}(x,\xi,t)\, \bar{N}(p_2)\, N(p_1) \Big),\end{aligned} \tag{8}$$

with $\bar{P} = p_1 + p_2$, $\Delta = p_2 - p_1$ and $\xi = -\Delta^+/2\bar{P}^+ \approx x_{Bj}/(2 - x_{Bj})$ (see e.g. [11] for details of the kinematics). In the case when the baryon state does not change, $A = B$, the corresponding GPDs are diagonal in flavor space,

$H^{q'q} \sim \delta_{q'q} H^q$, etc. In the general case, when $A \neq B$, in the right-hand side (r.h.s.) of Eqs. (7), (8) there might be extra structures, which vanish due to T-parity in the case $A = B$ [11]. In what follows we assume that the initial target A is either a proton or a neutron, and B belongs to the same lowest $SU(3)$ octet of baryons. In this case, all such terms are parametrically suppressed by the current quark mass m_q and vanish in the limit of exact $SU(3)$, so we will disregard them. In this special case, we may use $SU(3)$ relations and express the nondiagonal transitional GPDs as linear combinations of the GPDs of the proton H^q, E^q, $\tilde{H}^q$, $\tilde{E}^q$ [25], so (5) may be effectively rewritten as

$$\mathcal{A}_{\nu'0,\nu\alpha} = \int_{-1}^{+1} dx \sum_{q=u,d,s} \sum_{\lambda\lambda'} \mathcal{H}^q_{\nu',\nu} \mathcal{C}^q. \tag{9}$$

where $\mathcal{C}^q$ is the helicity independent part of the hard coefficient function. Its evaluation is quite straightforward, and in the leading order over α_s it gets contributions from the diagrams shown schematically in Figure 1. It has been studied both for pion electroproduction [19, 20, 31–35] and neutrinoproduction [21] (see also [29] for a discussion of higher twist corrections). In the next-to-leading order the evaluation becomes more complicated, and the corresponding diagrams are shown schematically in Figure 2.

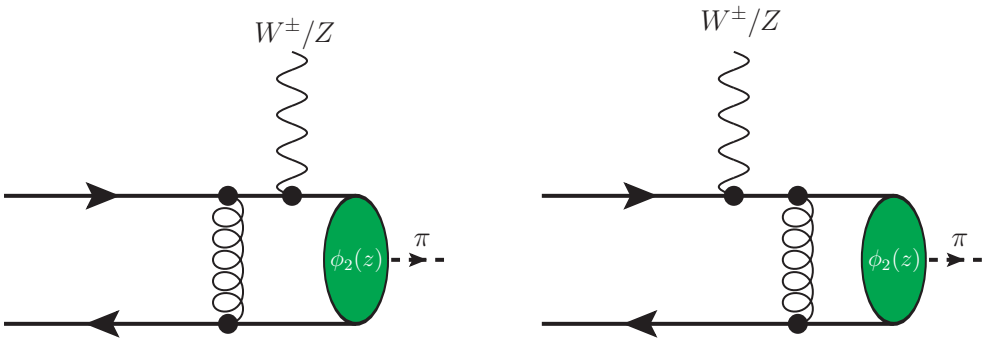

Figure 1: Leading-order contributions to the DVMP hard coefficient functions. Green blob stands for the pion wave function. Additional diagrams (not shown) may be obtained reversing directions of the quark lines.

Straightforward evaluation of the diagrams shown in the Figure 1 yields for the coefficient function

$$\mathcal{C}^q_{\lambda',\lambda\mu} = \eta^q_- c^{(2)}_- (x,\xi) + \mathrm{sgn}(\lambda) \eta^q_+ c^{(2)}_+ (x,\xi) + \mathcal{O}\left(\frac{m^2}{Q^2}\right) + \mathcal{O}\left(\alpha_s^2\left(\mu_R^2\right)\right) \tag{10}$$

where the process-dependent flavor factors $\eta^q_{V\pm}$, $\eta^q_{A\pm}$ are given in Table I [2], and we introduced shorthand notations

Table I: The flavor coefficients $\eta^q_\pm$ for several pion and kaon production processes discussed in this paper ($q = u, d, s, ...$). For the case of CC mediated processes, take $\eta^q_{V\pm} = \eta^q_\pm$, $\eta^q_{A\pm} = -\eta^q_\pm$. For the case of NC mediated processes, take g_q corresponding to g^q_V and g^q_A for helicity odd and helicity even GPDs respectively.

[2] As was discussed above, for processes with change of internal baryon structure, we use $SU(3)$ relations [25] which are valid up to corrections in current quark masses $\sim \mathcal{O}(m_q)$.

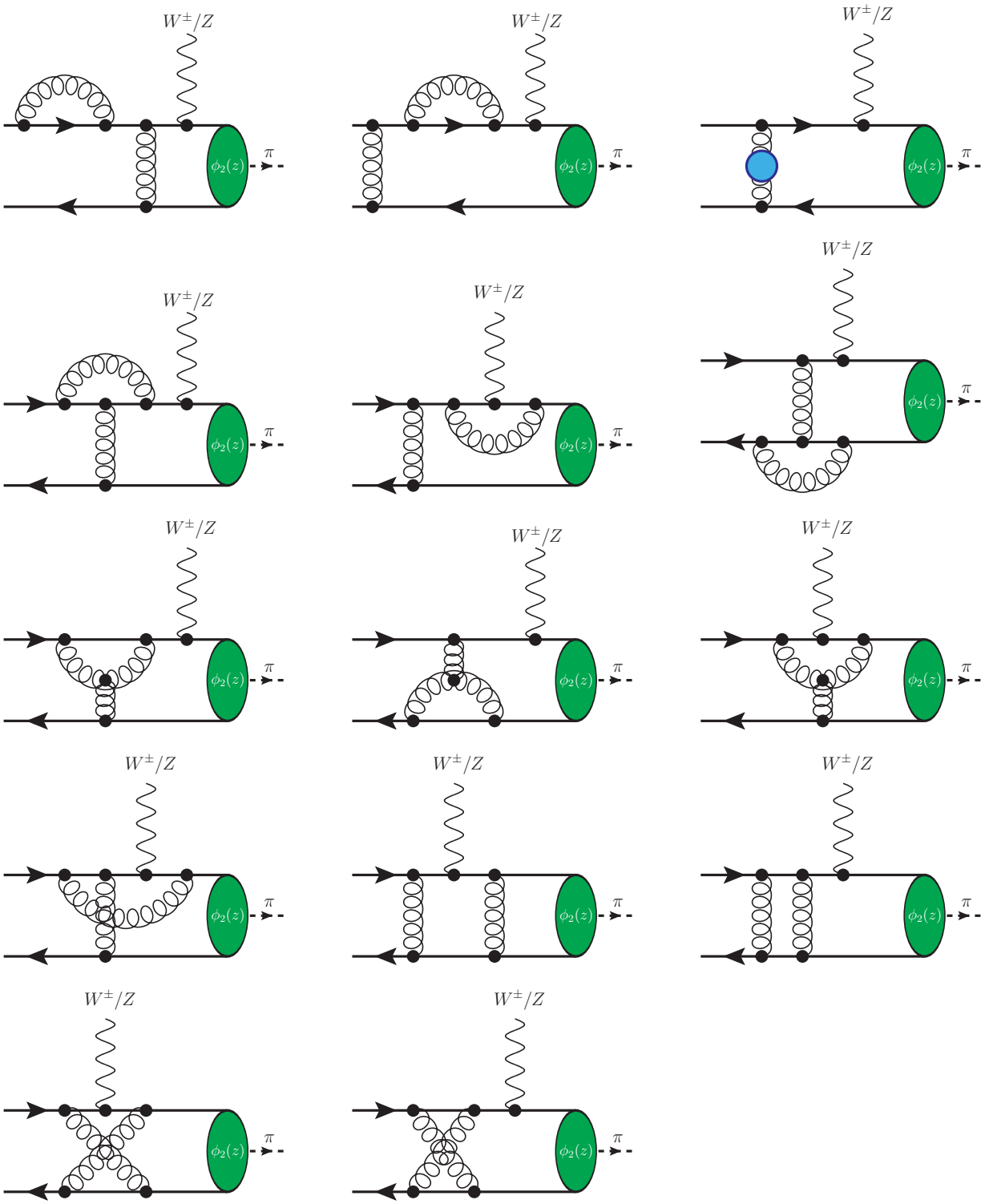

Figure 2: Next-to-leading-order contributions to the DVMP hard coefficient functions. Green blob stands for the pion wave function. Blue circle in the third diagram in the first line stands for all possible gluon mass corrections (sum of quark and gluon loops). Additional diagrams (not shown) may be obtained reversing directions of the quark lines.

Process	type	η_+^q	η_-^q
$\nu\, p \to \mu^- \pi^+ p$	CC	$V_{ud}\delta_{qu}$	$V_{ud}\delta_{qd}$
$\bar\nu\, p \to \mu^+ \pi^- p$	CC	$V_{ud}\delta_{qd}$	$V_{ud}\delta_{qu}$
$\bar\nu\, p \to \mu^+ \pi^0 n$	CC	$V_{ud}\frac{\delta_{qu}-\delta_{qd}}{\sqrt{2}}$	$-V_{ud}\frac{\delta_{qu}-\delta_{qd}}{\sqrt{2}}$
$\nu\, p \to \nu\, \pi^+ n$	NC	$g_d\,(\delta_{qu}-\delta_{qd})$	$g_u\,(\delta_{qu}-\delta_{qd})$
$\nu\, p \to \nu\, \pi^0 p$	NC	$\frac{g_u\delta_{qu}-g_d\delta_{qd}}{\sqrt{2}}$	$\frac{g_u\delta_{qu}-g_d\delta_{qd}}{\sqrt{2}}$

Process	type	η_+^q	η_-^q
$\nu\, n \to \mu^- \pi^+ n$	CC	$V_{ud}\delta_{qd}$	$V_{ud}\delta_{qu}$
$\bar\nu\, n \to \mu^+ \pi^- n$	CC	$V_{ud}\delta_{qu}$	$V_{ud}\delta_{qd}$
$\nu\, n \to \mu^- \pi^0 p$	CC	$-V_{ud}\frac{\delta_{qu}-\delta_{qd}}{\sqrt{2}}$	$V_{ud}\frac{\delta_{qu}-\delta_{qd}}{\sqrt{2}}$
$\nu\, n \to \nu\, \pi^- p$	NC	$g_u\,(\delta_{qu}-\delta_{qd})$	$g_d\,(\delta_{qu}-\delta_{qd})$
$\nu\, n \to \nu\, \pi^0 n$	NC	$\frac{g_u\delta_{qd}-g_d\delta_{qu}}{\sqrt{2}}$	$\frac{g_u\delta_{qd}-g_d\delta_{qu}}{\sqrt{2}}$

$\nu\, p \to \mu^- K^+ p$	CC	$V_{us}\delta_{qu}$	$V_{us}\delta_{qs}$
$\nu\, p \to \mu^- K^+ \Sigma^+$	CC	0	$-V_{ud}\,(\delta_{qd}-\delta_{qs})$
$\bar\nu\, n \to \mu^+ K^0 \Sigma^-$	CC	0	$-V_{ud}\,(\delta_{qu}-\delta_{qs})$

$\nu\, n \to \nu\, K^+ \Sigma^-$	NC	$-g_d\,(\delta_{qu}-\delta_{qs})$	$-g_u\,(\delta_{qu}-\delta_{qs})$
$\nu\, n \to \mu^- K^+ \Sigma^0$	CC	0	$-V_{ud}\frac{\delta_{qu}-\delta_{qs}}{\sqrt{2}}$
$\nu\, p \to \nu\, K^+ \Lambda$	NC	$-g_d\frac{2\delta_{qu}-\delta_{qd}-\delta_{qs}}{\sqrt{6}}$	$-g_u\frac{2\delta_{qu}-\delta_{qd}-\delta_{qs}}{\sqrt{6}}$

$$c_\pm^{(2)}\,(x,\xi) \;=\; \left(\int dz \frac{\phi_2(z)}{z}\right) \frac{8\pi i}{9}\,\frac{\alpha_s\left(\mu_R^2\right) f_M}{Q}\,\frac{1}{x\pm\xi\mp i0}\left(1+\frac{\alpha_s\left(\mu_r^2\right)}{2\pi}T^{(1)}\left(\frac{x\pm\xi}{2\xi},\, z\right)\right). \tag{11}$$

where $\phi_2(z)$ is the twist-2 $\pi-$or K-meson distribution amplitude (DA) defined as [36]

$$\phi_2\,(z) \;=\; \frac{1}{if_M\sqrt{2}}\int \frac{du}{2\pi} e^{i(z-0.5)u}\left\langle 0\left|\bar\psi\left(-\frac{u}{2}n\right)\hat n\gamma_5\psi\left(\frac{u}{2}n\right)\right|\pi(q)\right\rangle. \tag{12}$$

The function $T^{(1)}\,(v,\,z)$ in (11) encodes NLO corrections to the coefficient function. As was explained in [37–39] it is related by analytical continuation to the loop correction to $\bar qq$ scattering, and was evaluated and analyzed in detail in the context of NLO studies of the pion form factor (see [40, 41] for details and historical discussion). Explicitly, it is given by

$$\begin{aligned} T^{(1)}\,(v,\,z) = \frac{1}{2vz}\Bigg[&\frac{4}{3}\left(\left[3+\ln(v\,z)\right]\,\ln\left(\frac{Q^2}{\mu_F^2}\right)+\frac{1}{2}\ln^2(v\,z)+3\ln(v\,z)-\frac{\ln\bar v}{2\bar v}-\frac{\ln\bar z}{2\bar z}-\frac{14}{3}\right) \\ &+\beta_0\left(\frac{5}{3}-\ln(v\,z)-\ln\left(\frac{Q^2}{\mu_R^2}\right)\right) \\ &-\frac{1}{6}\Bigg(2\frac{\bar v\,v^2+\bar z\,z^2}{(v-z)^3}\left[\mathrm{Li}_2(\bar z)-\mathrm{Li}_2(\bar v)+\mathrm{Li}_2(v)-\mathrm{Li}_2(z)+\ln\bar v\,\ln z-\ln\bar z\,\ln v\right] \\ &+2\frac{v+z-2v\,z}{(v-z)^2}\ln(\bar v\bar z)+2\left[\mathrm{Li}_2(\bar z)+\mathrm{Li}_2(\bar v)-\mathrm{Li}_2(z)-\mathrm{Li}_2(v)+\ln\bar v\,\ln z+\ln\bar z\,\ln v\right] \\ &+\,4\frac{v\,z\,\ln(v\,z)}{(v-z)^2}-4\ln\bar v\,\ln\bar z-\frac{20}{3}\Bigg)\Bigg], \end{aligned} \tag{13}$$

where $\beta_0=\frac{11}{3}N_c-\frac{2}{3}N_f$, $\mathrm{Li}_2(z)$ is the dilogarithm function, and μ_R and μ_F are the renormalization and factorization scales respectively [3]. The correction $T^{(1)}\,(v,\,z)$ for small $v\approx 0$ ($x=\pm\xi\mp i0$) has an asymptotic behavior $\sim\ln^2 v$, which signals that a collinear approximation might be not valid near this point. To regularize the singularity, we may follow [18] and introduce a small transverse momentum $l_\perp$ of the quark inside a meson. Effectively, this corresponds to the introduction of a small infrared regularization in the region $v\sim l_\perp^2/Q^2$, a vanishingly small quantity in the Bjorken limit. However, a full evaluation of $T^{(1)}\,(v,\,z)$ beyond collinear approximation (taking into account all higher twist corrections) presents a challenging problem. Another possibility was suggested in [39], and corresponds to the absorption of the singular term by selecting a low renormalization scale $\mu_R^2\sim z\,v\,Q^2$. Near the points $x\approx\pm\xi$ the redefined scale μ_R drops to very small values, where nonperturbative effects become relevant. Only in the Bjorken limit ($Q^2\to\infty$) we may expect that details of regularization become irrelevant.

[3] For the sake of simplicity, we follow [39] and assume that the factorization scale μ_F is the same for both the generalized parton distribution and the pion distribution amplitude.

III. GPD AND DA PARAMETRIZATIONS

For the leading twist DA $\phi_{2\pi}(x)$, the currently available data on the meson photoproduction form factor $F_{\pi\gamma\gamma}\left(Q^2\right)$ are compatible with the asymptotic form $\phi_{as}(z) = 6\sqrt{2}f_\pi z(1-z)$, with a typical uncertainty in the minus-first moment of the order of $\sim 10\%$ (see e.g. [42, 43] and reviews in [44, 45]).

More than a dozen different parametrizations of GPDs have been proposed in the literature [7, 12, 35, 46–51]. While we neither endorse nor refute any of them, for the sake of concreteness we use the parametrization [33–35], which succeeded to describe HERA [52] and JLAB [33–35] data on electroproduction of different mesons, so it should provide a reasonable description of νDVMP. The parametrization is based on the Radyushkin's double distribution ansatz. It assumes additivity of the valence and sea parts of the GPDs,

$$H(x,\xi,t) = H_{val}(x,\xi,t) + H_{sea}(x,\xi,t), \tag{14}$$

which are defined as

$$H^q_{val} = \int_{|\alpha|+|\beta|\le 1} d\beta d\alpha \delta\left(\beta - x + \alpha\xi\right) \frac{3\theta(\beta)\left((1-|\beta|)^2-\alpha^2\right)}{4(1-|\beta|)^3} q_{val}(\beta) e^{(b_i - \alpha_i \ln|\beta|)t}, \tag{15}$$

$$H^q_{sea} = \int_{|\alpha|+|\beta|\le 1} d\beta d\alpha \delta\left(\beta - x + \alpha\xi\right) \frac{3\, sgn(\beta)\left((1-|\beta|)^2-\alpha^2\right)^2}{8(1-|\beta|)^5} q_{sea}(\beta) e^{(b_i - \alpha_i \ln|\beta|)t}, \tag{16}$$

and q_{val} and q_{sea} are the ordinary valence and sea components of the PDFs. The coefficients b_i, α_i, as well as the parametrization of the input PDFs $q(x)$, $\Delta q(x)$ and pseudo-PDFs $e(x)$, $\tilde{e}(x)$ (which correspond to the forward limit of the GPDs E, $\tilde{E}$), are discussed in [33–35]. The unpolarized PDFs $q(x)$ are adjusted to reproduce the CTEQ PDFs in the limited range $4 \lesssim Q^2 \lesssim 40$ GeV^2. Notice that in this model the sea is flavor symmetric for asymptotically large Q^2,

$$H^u_{sea} = H^d_{sea} = \kappa\left(Q^2\right) H^s_{sea}, \tag{17}$$

where

$$\kappa\left(Q^2\right) = 1 + \frac{0.68}{1 + 0.52\ln\left(Q^2/Q_0^2\right)}, \quad Q_0^2 = 4\,\text{GeV}^2.$$

The equality of the sea components of the light quarks in (17) should be considered only as a rough approximation, since in the forward limit the inequality $\bar{d} \neq \bar{u}$ was firmly established by the E866/NuSea experiment [53]. For this reason, predictions done with this parametrization of GPDs for the $p \rightleftarrows n$ transitions in the region $x_{Bj} \in (0.1...0.3)$ might slightly underestimate the data.

IV. NUMERICAL RESULTS AND DISCUSSION

In this section we would like to present numerical results for the next-to-leading order corrections to pion production using the Kroll-Goloskokov parametrization of GPDs [18, 33–35], briefly discussed in section III. Due to poor statistics of the neutrino-induced processes, it is challenging to measure the differential cross-section $d\sigma/dx_B dt\, dQ^2$, so we will restrict ourselves to the cross-section $d^2\sigma/dx_B dQ^2$. Using for reference the kinematics of MINERvA experiment [22], we assume that the average energy of the neutrino beam is 6 GeV. The predicted cross-section change only mildly when we smear out the cross-section with a realistic spectrum.

We would like to start a discussion about the dependence on the factorization scale μ_F, which separates hard and soft physics. As we can see from Figure 3, the results become independent on the factorization scale μ_F only at a sufficiently large $\mu_F \gtrsim 5$ GeV. Though the choice of factorization scale μ_F is arbitrary, a choice of a value significantly different from the virtuality Q could lead to large logarithms in higher order corrections. As was suggested in [37–39], varying the scale in the range $\mu_F \in (Q/2,\, 2Q)$, we can roughly estimate the error due to omitted higher order loop contributions.

In Figure 4 we show the predictions for the differential cross-section $d\sigma/dx_B dQ^2$ for charged and neutral pion production in several channels. For all cross-sections, at fixed neutrino energy E_ν and virtuality Q^2, we have a similar bump-like shape, which is explained by a competition of two factors. For small $x_B \sim Q^2/2m_N E_\nu$ the elasticity y defined in (4) approaches one, which causes a suppression due to a prefactor in (1). In the opposite limit, a suppression $\sim (1-x)^n$ is controlled by the implemented parametrization of GPD. As we can see from a comparison of the leading

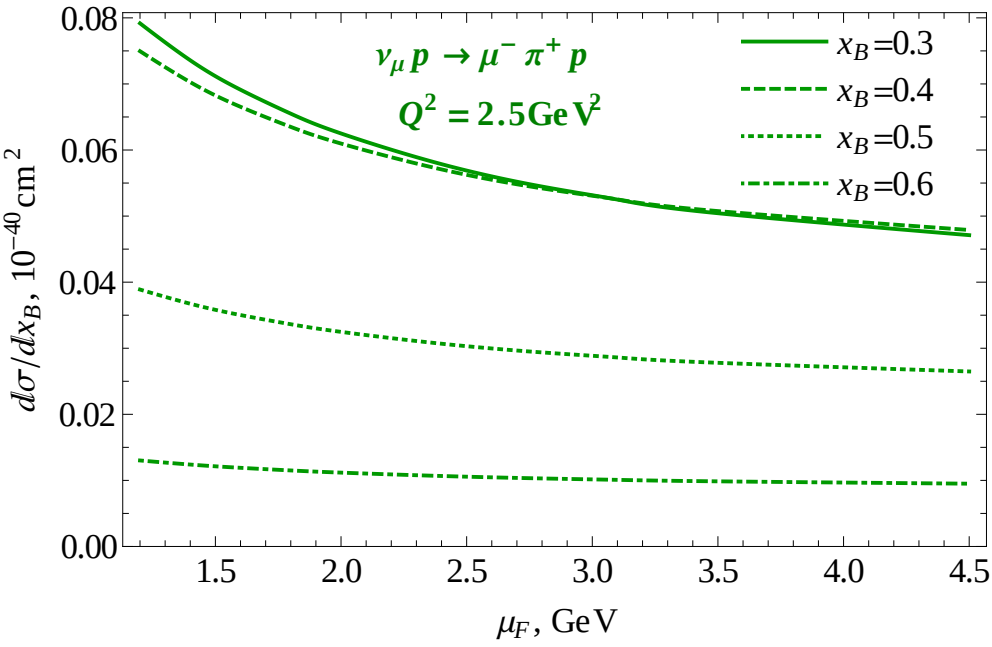

Figure 3: (color online) Factorization scale dependence of the charged current π^+ production for the process $\nu p \to \mu^- \pi^+ p$ for several values of x_B. Similar dependence is observed for all other processes.

order (dashed lines) and the full results (solid line surrounded by the green band), the next-to-leading order corrections are sizable and increase the full cross-section by ∼50%. In the charged current case, π^+ production on protons, the cross-section is even larger: as we explained in [21], in the leading order there is a partial cancellation of the s-channel and u-channel handbag contributions, which leads to a twice smaller cross-section compared to the same process on neutrons in leading order. However, for the next-to-leading order such cancellation no longer occurs, which explains the elevated NLO correction to the charged current π^+ production on protons.

Similarly, for the case of kaon production (see Figure 5), we observe that corrections are large. From the upper left plot we can see that Cabibbo suppressed ($\Delta S = 1$) K^+-production on the proton has extremely small cross-section, beyond the reach of ongoing and forthcoming experiments, and for this reason we do not consider other Cabibbo suppressed channels. The Cabbibo-allowed ($\Delta S = 0$) processes have an order of magnitude larger cross-sections and potentially could be used to test the poorly known strange quark GPD.

V. CONCLUSIONS

In this paper we estimated the contributions of the next-to-leading order corrections to pion and kaon production in neutrino-nucleus collisions. We found that these corrections increase the full cross-section by a factor of 1.5-2, and for this reason are important in the analysis of generalized parton distributions from the data. The NLO coefficient functions near the points $x \pm \xi$ have logarithmic behavior, which suggests that higher twist corrections in the NLO might be important, especially in the imaginary part. As was discussed in [29], such corrections generate the azimuthal angle dependence, which could be used to assess the size of these harmonics. However, at this moment a systematic evaluation of NLO corrections at twist 3 presents a challenging problem.

Qualitatively, our findings agree with large NLO corrections to meson *electro*production [37–39], deeply virtual Compton scattering [54–56] and timelike Compton scattering [57], expected in electron-induced processes. In view of this result, a future analysis of the next-to-next-to-leading order corrections is desirable. Our results are relevant for the analysis of pion and kaon production in the MINERVA experiment at FERMILAB as well as the planned Muon Collider/Neutrino Factory [58–60].

A code for the evaluation of the cross-sections, taking into account NLO corrections and employing various GPD models is available on demand.

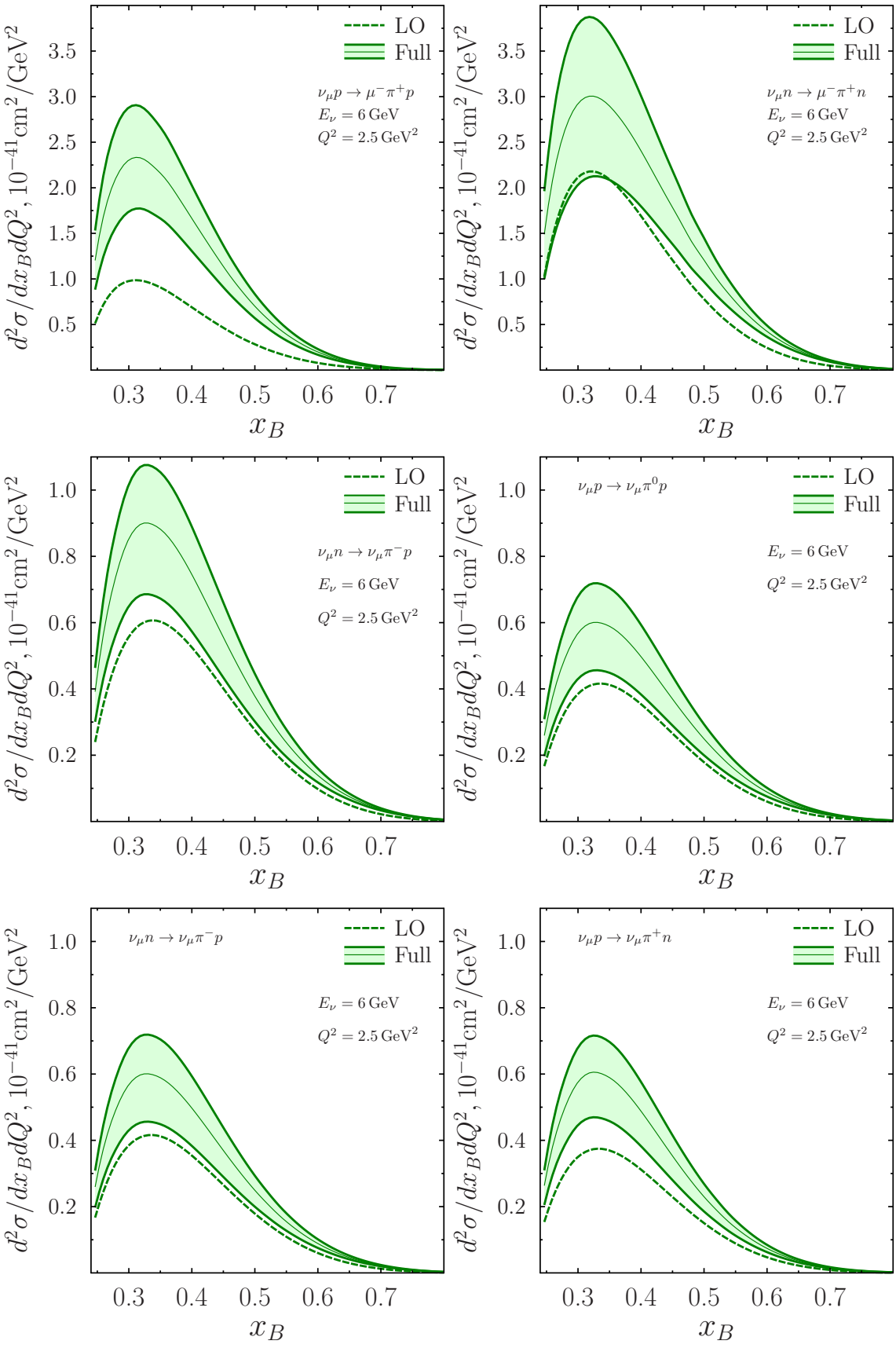

Figure 4: (color online) Pion production on nucleons, with neutral and charged currents at fixed energy neutrino beam ($E_\nu \approx 6$ GeV). The dashed line stands for the leading order evaluation, whereas the solid line surrounded by green error bands (marked as "Full") stands for the full result with NLO corrections. The width of the band represents the uncertainty due to the factorization scale choice $\mu_F \in (Q/2,\, 2Q)$, as explained in the text.

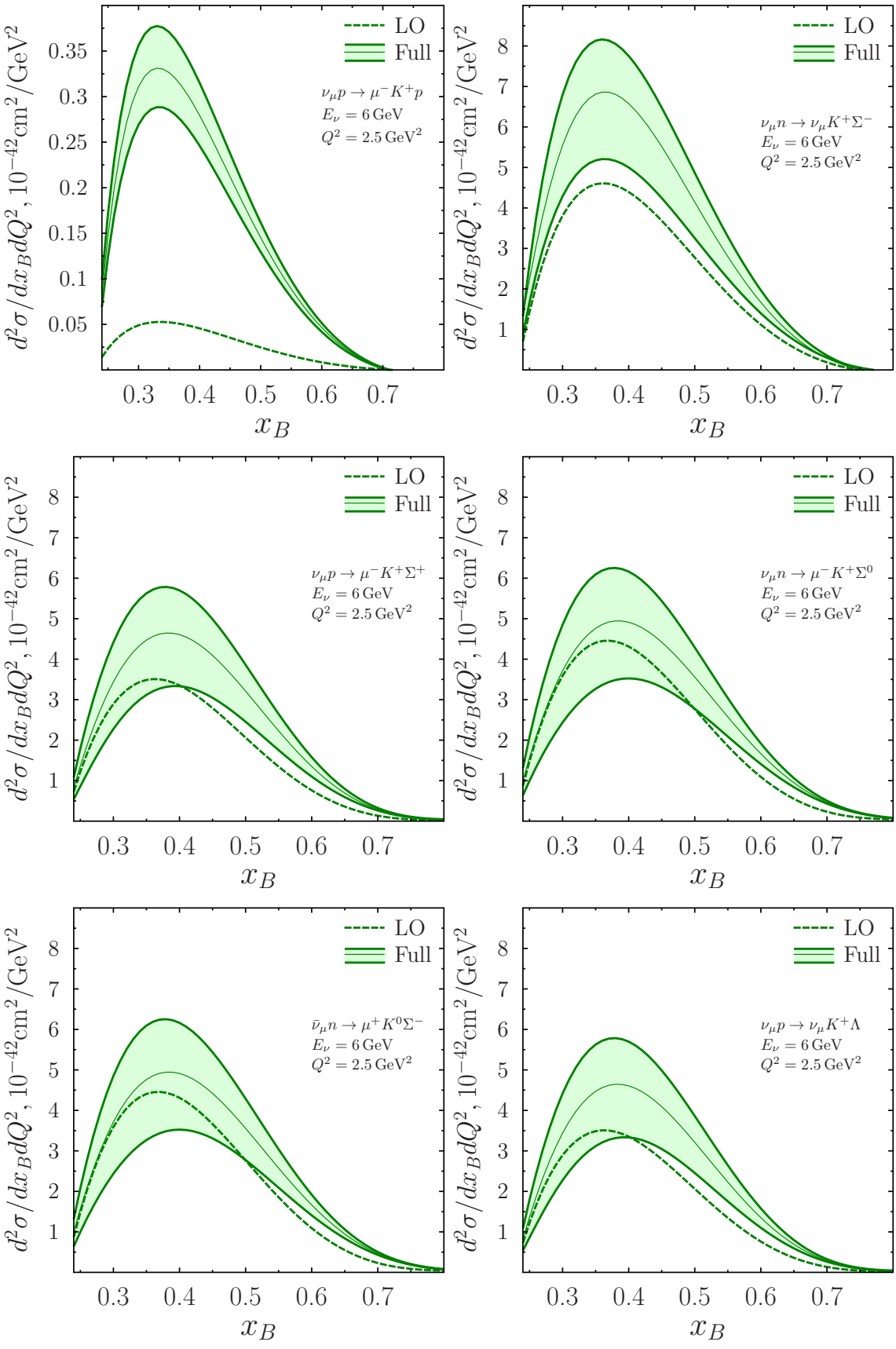
LO
Full
$\nu_\mu p \to \mu^- K^+ p$
$E_\nu = 6\,\mathrm{GeV}$
$Q^2 = 2.5\,\mathrm{GeV}^2$
$\nu_\mu n \to \nu_\mu K^+ \Sigma^-$
$\nu_\mu p \to \mu^- K^+ \Sigma^+$
$\nu_\mu n \to \mu^- K^+ \Sigma^0$
$\bar{\nu}_\mu n \to \mu^+ K^0 \Sigma^-$
$\nu_\mu p \to \nu_\mu K^+ \Lambda$
$d^2\sigma/dx_B dQ^2, 10^{-42}\mathrm{cm}^2/\mathrm{GeV}^2$
x_B

Figure 5: (color online) Selected neutral and charged current mediated kaon production cross-sections for fixed energy neutrino beam ($E_\nu \approx 6$ GeV). The dashed line stands for the leading order evaluation, whereas the solid line surrounded by green error bands (marked as "Full") stands for the full result, which takes into account NLO corrections. The width of the band represents the uncertainty due to the factorization scale choice $\mu_F \in (Q/2,\, 2Q)$, as explained in the text.

Acknowledgments

This research was partially supported by Proyecto Basal FB 0821 (Chile), the Fondecyt (Chile) grants 1140390 and 1140377, CONICYT (Chile) grant PIA ACT1413. Powered@NLHPC: This research was partially supported by the supercomputing infrastructure of the NLHPC (ECM-02). Also, we thank Yuri Ivanov for technical support of the USM HPC cluster where part of evaluations were done.

[1] X. D. Ji and J. Osborne, Phys. Rev. D **58** (1998) 094018 [arXiv:hep-ph/9801260].
[2] J. C. Collins and A. Freund, Phys. Rev. D **59**, 074009 (1999).
[3] D. Mueller, D. Robaschik, B. Geyer, F. M. Dittes and J. Horejsi, Fortsch. Phys. **42**, 101 (1994) [arXiv:hep-ph/9812448].
[4] X. D. Ji, Phys. Rev. D **55**, 7114 (1997).
[5] X. D. Ji, J. Phys. G **24**, 1181 (1998) [arXiv:hep-ph/9807358].
[6] A. V. Radyushkin, Phys. Lett. B **380**, 417 (1996) [arXiv:hep-ph/9604317].
[7] A. V. Radyushkin, Phys. Rev. D **56**, 5524 (1997).
[8] A. V. Radyushkin, arXiv:hep-ph/0101225.
[9] J. C. Collins, L. Frankfurt and M. Strikman, Phys. Rev. D **56**, 2982 (1997).
[10] S. J. Brodsky, L. Frankfurt, J. F. Gunion, A. H. Mueller and M. Strikman, Phys. Rev. D **50**, 3134 (1994).
[11] K. Goeke, M. V. Polyakov and M. Vanderhaeghen, Prog. Part. Nucl. Phys. **47**, 401 (2001) [arXiv:hep-ph/0106012].
[12] M. Diehl, T. Feldmann, R. Jakob and P. Kroll, Nucl. Phys. B **596**, 33 (2001) [Erratum-ibid. B **605**, 647 (2001)] [arXiv:hep-ph/0009255].
[13] A. V. Belitsky, D. Mueller and A. Kirchner, Nucl. Phys. B **629**, 323 (2002) [arXiv:hep-ph/0112108].
[14] M. Diehl, Phys. Rept. **388**, 41 (2003) [arXiv:hep-ph/0307382].
[15] A. V. Belitsky and A. V. Radyushkin, Phys. Rept. **418**, 1 (2005) [arXiv:hep-ph/0504030].
[16] V. Kubarovsky [CLAS Collaboration], Nucl. Phys. Proc. Suppl. **219-220**, 118 (2011).
[17] S. Ahmad, G. R. Goldstein and S. Liuti, Phys. Rev. D **79** (2009) 054014 [arXiv:0805.3568 [hep-ph]].
[18] S. V. Goloskokov and P. Kroll, Eur. Phys. J. C **65**, 137 (2010) [arXiv:0906.0460 [hep-ph]].
[19] S. V. Goloskokov and P. Kroll, Eur. Phys. J. A **47**, 112 (2011) [arXiv:1106.4897 [hep-ph]].
[20] G. R. Goldstein, J. O. G. Hernandez and S. Liuti, arXiv:1201.6088 [hep-ph].
[21] B. Z. Kopeliovich, I. Schmidt and M. Siddikov, Phys. Rev. D **86** (2012), 113018 [arXiv:1210.4825 [hep-ph]].
[22] D. Drakoulakos *et al.* [Minerva Collaboration], hep-ex/0405002.
[23] B. Z. Kopeliovich, I. Schmidt and M. Siddikov, Phys. Rev. D **89**, no. 5, 053001 (2014) [arXiv:1401.1547 [hep-ph]].
[24] G. R. Goldstein, O. G. Hernandez, S. Liuti and T. McAskill, AIP Conf. Proc. **1222**, 248 (2010) [arXiv:0911.0455 [hep-ph]].
[25] L. L. Frankfurt, P. V. Pobylitsa, M. V. Polyakov and M. Strikman, Phys. Rev. D **60** (1999) 014010 [hep-ph/9901429].
[26] B. Pire and L. Szymanowski, Phys. Rev. Lett. **115** (2015), 092001 [arXiv:1505.00917 [hep-ph]].
[27] B. Pire and L. Szymanowski, Acta Phys. Polon. Supp. **8**, 883 (2015) [arXiv:1510.01869 [hep-ph]].
[28] B. Pire, L. Szymanowski and J. Wagner, EPJ Web Conf. **112**, 01018 (2016) [arXiv:1601.07666 [hep-ph]].
[29] B. Z. Kopeliovich, I. Schmidt and M. Siddikov, Phys. Rev. D **87**, 033008 (2013) [arXiv:1301.7014 [hep-ph]].
[30] I. Schmidt and M. Siddikov, Phys. Rev. D **91**, no. 7, 073002 (2015) [arXiv:1501.04306 [hep-ph]].
[31] M. Vanderhaeghen, P. A. M. Guichon and M. Guidal, Phys. Rev. Lett. **80**, 5064 (1998).
[32] L. Mankiewicz, G. Piller and A. Radyushkin, **10**, 307 (1999) [hep-ph/9812467].
[33] S. V. Goloskokov and P. Kroll, Eur. Phys. J. C **50**, 829 (2007) [hep-ph/0611290].
[34] S. V. Goloskokov and P. Kroll, Eur. Phys. J. C **53**, 367 (2008) [arXiv:0708.3569 [hep-ph]].
[35] S. V. Goloskokov and P. Kroll, Eur. Phys. J. C **59** (2009) 809 [arXiv:0809.4126 [hep-ph]].
[36] B. Z. Kopeliovich, Iván Schmidt and M. Siddikov, Nucl. Phys. A **918**, 41 (2013) [arXiv:1108.5654 [hep-ph]].
[37] A. V. Belitsky and D. Mueller, Phys. Lett. B **513**, 349 (2001) [hep-ph/0105046].
[38] D. Y. Ivanov, L. Szymanowski and G. Krasnikov, JETP Lett. **80**, 226 (2004) [Pisma Zh. Eksp. Teor. Fiz. **80**, 255 (2004)] Erratum: [JETP Lett. **101**, no. 12, 844 (2015)] , [hep-ph/0407207].
[39] M. Diehl and W. Kugler, Eur. Phys. J. C **52**, 933 (2007) [arXiv:0708.1121 [hep-ph]].
[40] E. Braaten and S. M. Tse, Phys. Rev. D **35**, 2255 (1987).
[41] B. Melic, B. Nizic and K.˜Passek, Phys. Rev. **60**, 074004 (1999) [hep-ph/9802204].
[42] A. V. Pimikov, A. P. Bakulev, S. V. Mikhailov and N. G. Stefanis, arXiv:1208.4754 [hep-ph].
[43] A. P. Bakulev, S. V. Mikhailov, A. V. Pimikov and N. G. Stefanis, Phys. Rev. D **86** (2012) 031501 [arXiv:1205.3770 [hep-ph]].
[44] S. J. Brodsky, F. -G. Cao and G. F. de Teramond, Phys. Rev. D **84**, 075012 (2011) [arXiv:1105.3999 [hep-ph]].
[45] S. J. Brodsky, F. -G. Cao and G. F. de Teramond, Phys. Rev. D **84**, 033001 (2011) [arXiv:1104.3364 [hep-ph]].
[46] K. Kumericki, D. Muller and A. Schafer, JHEP **1107**, 073 (2011) [arXiv:1106.2808 [hep-ph]].
[47] M. Guidal, Phys. Lett. B **693**, 17 (2010) [arXiv:1005.4922 [hep-ph]].
[48] M. V. Polyakov and K. M. Semenov-Tian-Shansky, Eur. Phys. J. A **40**, 181 (2009) [arXiv:0811.2901 [hep-ph]].
[49] M. V. Polyakov and A. G. Shuvaev, hep-ph/0207153.
[50] A. Freund, M. McDermott and M. Strikman, Phys. Rev. D **67**, 036001 (2003) [hep-ph/0208160].

[51] G. R. Goldstein, J. O. G. Hernandez and S. Liuti, arXiv:1311.0483 [hep-ph].
[52] F. D. Aaron *et al.* [H1 Collaboration], JHEP **1005** (2010) 032 [arXiv:0910.5831 [hep-ex]].Phys. Rev. D **82**, 033001 (2010) [arXiv:1004.5484 [hep-ph]].
[53] E. A. Hawker *et al.* [FNAL E866/NuSea Collaboration], Phys. Rev. Lett. **80** (1998) 3715 [hep-ex/9803011].
[54] A. Freund and M. McDermott, Eur. Phys. J. C **23**, 651 (2002) [hep-ph/0111472].
[55] A. V. Belitsky, D. Mueller, L. Niedermeier and A. Schafer, Phys. Lett. B **474**, 163 (2000) [hep-ph/9908337].
[56] A. V. Belitsky and D. Mueller, Phys. Lett. B **417**, 129 (1998) [hep-ph/9709379].
[57] B. Pire, L. Szymanowski and J. Wagner, Phys. Rev. D **83**, 034009 (2011) [arXiv:1101.0555 [hep-ph]].
[58] J. C. Gallardo, R. B. Palmer, A. V. Tollestrup, A. M. Sessler, A. N. Skrinsky, C. Ankenbrandt, S. Geer and J. Griffin *et al.*, eConf C **960625** (1996) R4.
[59] C. M. Ankenbrandt, M. Atac, B. Autin, V. I. Balbekov, V. D. Barger, O. Benary, J. S. Berg and M. S. Berger *et al.*, Phys. Rev. ST Accel. Beams **2** (1999) 081001 [physics/9901022].
[60] M. M. Alsharoa *et al.* [Muon Collider/Neutrino Factory Collaboration], Phys. Rev. ST Accel. Beams **6** (2003) 081001 [hep-ex/0207031].